Heliyon 7 (2021) e07974

Contents lists available at ScienceDirect

Heliyon

journal homepage: www.cell.com/heliyon

Research article

Natural zeolite as a chromium VI removal agent in tannery effluents

Ana María Álvarez [a], Darío Bolaños Guerrón [a,b], Carolina Montero Calderón [a,c,*]

[a] Universidad de las Fuerzas Armadas "ESPE" - Departamento de Ciencias de la Tierra y la Construcción – Maestría en Sistemas de Gestión Ambiental, Sangolquí, Ecuador
[b] Universidad de las Fuerzas Armadas "ESPE" - Centro de Nanociencia y Nanotecnología (CENCINAT), Sangolquí, Ecuador
[c] Facultad de Ingeniería Química, Universidad Central del Ecuador, Quito, Ecuador

ARTICLE INFO

Keywords:
Activation
Adsorption
Tannery effluent
Zeolite

ABSTRACT

This study concerns Cr(VI) removal using zeolites in a batch system for tannery effluent. In the initial stage, natural zeolite (ZN) and synthetic zeolite (ZS) were characterized, obtaining a Si/Al ratio of 4.64 and 1.60, and with predominant clinoptilolite and faujasite phases, the surface area of 9.34 and 25.82 m^2/g and cation exchange capacity of 84.05 and 188.72 meq/100 g, respectively. Subsequently, ZN and ZS were activated with HCl and NaOH. Through preliminary tests, with a solution of $K_2Cr_2O_7$, it was determined that the highest Cr(VI) removal for both, ZN and ZS, was with NaOH activation, obtaining 82 and 56% removal, respectively. According to Ecuadorian regulations, the Cr(VI) concentration exceeds the maximum permissible limits on the tannery effluent. For this effluent, it was determined that the highest Cr(VI) removal, 45%, is obtained with 1 g of ZN activated with NaOH and 100 mL of effluent. With ZN-NaOH, removal tests were carried out in a fixed bed with 5, 10, and 20 g of natural zeolite. The natural zeolite also has chromium removal capacity in the bed system, achieving similar removals to those obtained in the batch experiments, but decreasing the treatment time. Thus, both natural and synthetic zeolites can remove Cr(VI) in tannery effluents, achieving this effluent with permissible limits.

1. Introduction

In Ecuador, the leather industry has grown 8.6 % in the last decade; the province with the most significant leather production is Tungurahua, 76 % of the total [1]. However, despite the economic benefits, the leather industry generates an environmental impact as effluent parameters such as COD, BOD_5, suspended solids, and sulfates often do not comply with regulations [2].

In the leather industry, the most widely used substances are chromium salts. However, 15% of these salts also react with the leather, and the non-reacted chemicals (85%) are not absorbed into the leather, which generates significant volumes of liquid effluents with a complex combination of organic and inorganic compounds [3]. Conventional wastewater treatments, such as electrochemical [4], photocatalysis [5] and anaerobic reactors [6]; and the use of natural materials, such as adsorbents [7, 8], have been proved to restore tannery effluents. In addition, there is the possibility of an oxidation process of Cr (III) to Cr (VI), which is approximately 100 times more toxic and 1000 times more mutagenic than Cr (III), being also carcinogenic because as it modifies the DNA transcription process causing chromosomal aberrations [9].

Chromium VI is dangerous; it is soluble and mobile in water. It affects the consumption rates of animal and plant cells, and it is available to living organisms, it can enter the body via several routes, consumption, epidermal adhesion, inhalation and absorption in plants and roots; it shortens the sprouting of seeds and delays photosynthesis and enzyme action in algae due to the presence of Chromium VI in concentrations as low as 10 ppm [10]. On the other hand, natural zeolites have different characteristics attributed to the geological formations in different places, so each zeolite has distinct characteristics. However, most of them are suitable for removing heavy metals, and the activation of their pores improves their efficiency through the addition of acids, calcination, etc [9, 11, 12].

Some previous works have focused on the adsorption to chromium with different materials. Hydrogels derived from gelatin and eucalyptus residues indicated that the gelatin hydrogel and composite hydrogels presented great potential for chromium (VI) adsorption in solution with an adsorption value of 12.3 mg/g [13]. A metal-organic framework synthesized via a hydrothermal route and HF mineralizing agent [14] has been used to remove lead (II) and chromium (VI). It was observed that solution pH is a significant operating factor affecting the acid-base

* Corresponding author.
E-mail address: cdmontero@uce.edu.ec (C. Montero Calderón).

https://doi.org/10.1016/j.heliyon.2021.e07974
Received 2 July 2021; Received in revised form 12 August 2021; Accepted 7 September 2021

property of the sorbent surface and accordingly has an important role in the adsorption efficiency; in this work, 30.45 mg/g of Cr(VI) was removed. Different types of natural unconsolidated sediments in a system were studied through batch and column experiments [15]; it was concluded that the increase in the solution pH and solid/solution ratio resulted in a decrease in the adsorption of Cr (VI). In this work 15–85% of Cr(VI) was removed. On the other hand, novel materials have been developed as innovative adsorption materials to remove dyes [16, 17, 18, 19] and wastewater pollutants [20].

Due to its toxicity, Cr (VI) must be removed from tannery effluents before discharge. One of the most recently used methods is adsorption with natural materials; in our country some zeolites formations [21] can be used for pollutant removal. Due to the high natural and synthetic availability of zeolites and the relatively low cost of the adsorption processes; this work focuses on the study of chromium VI sorption in effluents derived from a real tannery located in Tungurahua Ecuador.

2. Experimental section

2.1. Zeolites

Natural zeolites and synthetic zeolites were used. The zeolites were collected at sampling points located within the northern foothills of the Chongón-Colonche mountain range, Guayas Ecuador; the zeolite samples were named ZN01, ZN02, and ZN03, respectively. The synthetic zeolite, from Meiqi Industry & Trade Co., LTD (China), was named ZS.

2.2. Zeolites characterization

The chemical composition of the oxides (%wt) in the natural and synthetic zeolites was determined by X-ray fluorescence (XRF) in a Bruker S8 Tiger at the ex-Instituto Nacional Geológico Minero Metalúrgico del Ecuador. The surface area was determined by the BET method in a Micromeritics Autochem 2920 in the Laboratorio de Investigación, Facultad de Ingeniería Química, Universidad Central del Ecuador.

Bulk density (ρ_b) was determined by the air displacement method used [22] in Eq. (1):

$$\rho_b = \frac{mass\ of\ the\ sample}{volume\ of\ the\ sample\ after\ displacement} \quad [1]$$

The real density (ρ_r) was determined using Eq. (2) [22]:

$$\rho_r = \frac{(W_3 - W_1)}{(W_2 - W_1) - (W_4 - W_3)} \times \rho_{water} \quad [2]$$

where W_1 denotes weight of a dry 50 mL flask; W_2 denotes the weight of the flask filled with distilled water; W_3 denotes the weight of the flask with 1 g of sample; W_4 denotes the weight of the flask with 1 g of sample and filled with distilled water; ρ_{water} denotes the density of the water.

The porosity of the zeolites was determined by the relationship shown in Eq. (3) [22]:

$$\%\,P = \left[1 - \left(\frac{\rho_b}{\rho_r}\right)\right] \times 100 \quad [3]$$

P is the porosity.

The identification of mineral phases was carried out by X-ray diffraction (XRD) with the Advanced Bruker Model D8 equipment at the ex-Instituto Nacional de Investigación Geológico Minero Metalúrgico-Ecuador.

2.3. Zeolite exchange capacity

The theoretical exchange capacity (TEC) was determined using Eq. (4) [23]:

$$TEC = \frac{e_{Al} \times 1000}{M_w} \times 100 \quad [4]$$

where e_{Al} denotes the aluminum atoms in the zeolite formula (equivalents/mole), M_w denotes the molecular mass of the zeolite (g/mol), 1000 denotes the factor to express the result in meq; and 100 to refer the result of 100 g of zeolite.

The cation exchange capacity- (CEC meq/100 g) was determined using the sodium hydroxide method [24]; Eq. (5) was used:

$$CEC = \frac{(V_1 - V_2) \times M \times 200}{P_M} \times K \quad [5]$$

V_1 denotes the arithmetic mean of the volumes of sodium hydroxide solution consumed in the blank assay titration (mL); V_2 denotes the volume of sodium hydroxide consumed in the sample titration (mL); M denotes the molarity of the sodium hydroxide solution (0.1M), and P_M denotes the sample weight (g).

The percentage of moisture (%H) was determined by Eq. (6):

$$\%H = \frac{P_1 - P_2}{P_M} \times 100 \quad [6]$$

The recalculation coefficient for the dry sample was determined by Eq. (7):

$$K = \frac{100}{100 - \%H} \quad [7]$$

P_1 denotes the weight of the sample plus the initial filter weight; P_2 denotes the weight of the dried sample plus the filter weight; and P_M denotes the initial sample's weight. The experiments were carried out in Departamento de Ciencias de la Tierra y Construcción-ESPE.

2.4. Characterization of tannery effluents

The adsorption process was performed with zeolites in wastewater samples provided by a tannery located in Tungurahua, Ecuador.

The determination of hydrogen potential (pH) and conductivity was measured with HACH HQ40D equipment by the tannery industry. From the conductivity, the total dissolved solids (TDS) were determined using Eqs. (8) and (9) [25]:

$$TDS = EC \times 800 \quad EC > 5\frac{dS}{m} \quad [8]$$

$$TDS = EC \times 640 \quad EC < 5\frac{dS}{m} \quad [9]$$

TDS denotes the total dissolved solids (mg/L), and EC denotes the electrical conductivity (dS/m).

The chemical oxygen demand (COD) was determined with a HACH DR 2800 spectrophotometer by the tannery industry.

Chromium (VI) was quantified by UV-VIS spectrophotometry, using the 3500-CrB method, at a wavelength of 540 nm [26]. A HANNA-HI 83099 + COD photometer was used, the concentration of Chromium (VI) was determined using the diphenylcarbazide colorimetric method [27].

2.5. Activation of zeolite

Before the adsorption process, the zeolites were activated in acid and basic medium. The activation of the zeolite in an acid medium was performed with an HCl solution (0.5M) using a 1:3 acid zeolite ratio for 1 h at 70 °C. The zeolite was subsequently washed with distilled water for 1 h at 70 °C, dried at 105 °C, and calcined at 350 °C for 2 h [28]. Activation in the basic medium was performed with NaOH (1 N) solution, and the zeolite was mixed with the basic solution in a 1:3 ratio; the mixture was stirred for 2 h at 70 °C. Then, the zeolite was washed with distilled water

to neutral pH. Finally, the zeolite was dried at 110 °C for 4 h and placed in a desiccator [29]. These experiments were done Departamento de Ciencias de la Tierra y Construcción-ESPE.

2.6. Chromium (VI) removal with zeolite

It has been reported that there is a dependence of the removal efficiency and adsorption capacity of Cr (VI) on the particle size of the zeolite. Homaid and Hamdo (2014) delimited a particle size of 75 μm [30]; therefore, natural and synthetic zeolite with a particle size between 63 and 75 μm were used for this work. Tests were carried out with a potassium dichromate solution ($K_2Cr_2O_7$) with concentrations of 0.9 and 0.7 mg/L, with a volume-mass ratio of 100 mL per 1 g of zeolite [31].

The solutions were placed in beakers under constant agitation; the operating conditions were an adsorption time of 3 h and agitation speed of 250 rpm, and experiments were performed with 50, 100, and 150 mL of solution. With the best results of chromium removal from the potassium dichromate solution, tests were carried out with tannery effluent with a Cr (VI) concentration of 0.6 mg/L. The percentage removal of Cr (VI) was determined with Eq. (10) [32]:

$$\%\ Removal = \frac{(C_i - C_f)}{C_i} \times 100 \quad [10]$$

C_i: initial Cr (VI) concentration; C_f: final Cr (VI) concentration after adsorption.

In addition, in order to propose a full-scale adsorption system, adsorption tests were carried out on a packed bed in a glass column with an internal diameter of 1.9 cm and external diameter of 2.3 cm, the initial influent concentration of 0.6 mg/L and a zeolite bed with a particle size of 1.4–2.4 mm [33]. Bed heights of 2.0, 3.9, and 7.2 cm were prepared using 5, 10, and 20 g of the zeolite material and were tested with an effluent volume of 50 mL. The experiments were carried out in Laboratorio de Medio Ambiente del Departamento de Ciencias de la Tierra y Construcción-ESPE.

3. Results and discussion

3.1. Physical-chemical zeolite properties

The composition in the form of oxides of the natural (ZN) and synthetic (ZS) zeolites are given in Table 1:

The results of oxide composition show that there is a majority presence of silica and alumina for both types of zeolites. The natural zeolite (ZN) also presents significant percentages of calcium, iron, and magnesium, while in the synthetic zeolite (ZS), magnesium presents a value of over 2%. Magnesium, calcium, and potassium can be exchanged with other ions, metallic and non-metallic, while the rest of the elements can be considered impurities that occupy the zeolite pores. Table 2 presents the Si/Al ratio for natural and synthetic zeolites, quantified from the percentages of Al_2O_3 and SiO_2.

Zeolites such as Ca-heulandite and Ca-clinoptilolite from a near geological formation in Guayas Ecuador, presented, Si/Al between 3:30 and 4.35. Zeolites with a higher Si/Al ratio have better stability in an acid medium and lower hydrophilicity as a reduced amount of Al causes the negative charges to decrease. Therefore, there is a minor attraction to the dipoles of the water molecule [34].

Table 2. Si/Al ratio of natural (ZN) and synthetic zeolites (ZS).

Zeolite	Si/Al
ZN01	3.55
ZN02	3.51
ZN03	4.64
ZS01	1.60

Zeolites with lower Si/Al have more aluminum in the structure; due to the presence of a high amount of aluminum have a high cation exchange capacity [35]. Therefore, they should compensate more charge with cations located outside of the net; as a result, they have more spots where water would interact with zeolite, increasing the hydrophilicity of the material [36]. In this regard, the natural zeolite would have better stability in an acid medium, so the ZN03 zeolite with a Si/Al ratio of 4.64 was considered for developing this work. Comparing the Si/Al = 4 ratio results, which correspond to a heulandite zeolite, and the Si/Al ratio >4 to a clinoptilolite, the results show that the ZN03 zeolite with a Si/Al ratio of 4.64 was considered for the development of the process [37]; it can be inferred that ZN03 could be one of these two types of zeolite.

The surface area results indicate that the synthetic zeolite ZS01 has a surface area of 25.82 m^2/g, a relatively low value since synthetic zeolites can have areas up to 780 m^2/g [38]. For ZN03, a surface area of 9.34 m^2/g was obtained. For natural zeolites, surface areas between 7.1 for potassic heulandite zeolite and 3.7 m^2/g for potassic clinoptilolite were reported [39], lower values than the surface area of the ZN03. Surface area values of 31.8, 30.8, and 18.4 m^2/g reported [40] for natural zeolites with mostly clinoptilolite and traces of modernite from deposits located in Mexico. These variations of the specific surface areas are probably due to the origin of the natural zeolites and traces of other oxides that obstruct the pores, as reported in the XRF results shown in Table 1.

The density results of the zeolites are presented in Table 3. The density of the natural zeolite ZN03 is slightly higher than that of the synthetic zeolite ZS01; a higher density generates fewer hollow spaces in the zeolites which allows the production of more active sites for adsorption. Therefore, the natural zeolite has a higher porosity percentage which involves a higher internal surface. Low densities were reported (0.8 g/cm^3) and porosities higher than 65 %, so due to the similarity of the reported values, it is ratified that the natural zeolite ZN03 would be of this type [41].

The mineral phases reported in Table 4 were determined by X-Ray diffraction (XRD). The natural zeolite (ZN03) has a majority composition

Table 3. Physical properties of studied zeolites.

Zeolites	ρ_b (g/cm^3)	ρ_r (g/cm^3)	%P
ZN03	0.84	2.26	62.98
ZS01	0.78	1.88	58.45

ρ_b: bulk density; ρ_r: real density; %P: porosity percentage.

Table 1. Composition of oxides (%wt) in natural and synthetic zeolites determined by XRF.

Zeolite	Na_2O	MgO	Al_2O_3	SiO_2	P_2O_5	SO_3	K_2O	CaO	TiO_2	Mn_2O_3	Fe_2O_3
ZN01	2.43	2.74	12.09	48.74	0.20	<0.05	0.83	8.12	0.70	0.18	7.64
ZN02	1.68	3.13	12.64	50.21	0.19	<0.05	0.71	5.74	0.70	0.15	7.40
ZN03	0.99	2.10	11.04	58.08	0.19	<0.05	0.70	4.84	0.43	0.08	4.25
ZS01	>11.00	2.55	24.04	43.45	0.06	<0.05	0.65	0.44	0.11	0.03	0.73

ZN01: natural zeolite 01; ZN02: natural zeolite 02; ZS01: synthetic zeolite 01.

Table 4. Zeolite mineral phases identified by XRD.

Zeolites	Quartz (%)	Plagioclase group (Anorthite) (%)	Feldespates (Orthoclase, Microcline, Sanidine) (%)	Muscovite (%)	Clinoptilolite, Heulandite (%)	Stilbite (%)	Faujasite (%)
ZN03	18.1	20.8	-	2.6	43.9	10.8	3.8
ZS01	6.2	-	37.4	-	-	-	56.4

of clinoptilolite/heulandite. In addition, based on the results of XRF data (Table 1), it comprises high silica heulandite with a percentage mass of Ca>>Na> K and low silica clinoptilolite (Ca-Clinoptilolite) considering the Si/Al ratio of 4.64 % [42]. The synthetic zeolite (ZS01) has a majority faujasite composition, consistent with the Si/Al = 1.60 ratio corresponding to this type of zeolite [39].

3.2. Quantification of cation exchange capacity (CEC)

The theoretical exchange capacity (TEC) was determined based on the theoretical formulas. Table 5 presents the results, which show that the theoretical exchange capacity of the synthetic zeolite ZS01 is 2.17 times higher than that of the natural zeolite ZN03.

Table 5 reports the cation exchange capacity (CEC) results, which also replicate the behavior of the synthetic zeolite with the highest cation exchange capacity. The synthetic zeolites with a low Si/Al ratio have a high cation exchange capacity [43], which was observed in this case for ZS01 with a 2.24 times higher cation exchange capacity than the natural zeolite ZN03. In this case, the faujasite-type synthetic zeolite has a higher cation exchange capacity than the clinoptilolite-type natural zeolite. The cation exchange capacity is directly proportional to the number of Al atoms present in the tetrahedral structure; the Si/Al ratio >4 results in a relatively low ion exchange capacity, the highest value of which belongs to ZN03 [41], in addition to the presence of impurities and quartz, as in the case of natural zeolites. Other natural materials, such as kaolinite, used in adsorption on direct brown dye reported CEC values between 80 and 179 meq/100 g [44].

3.3. Determination of physicochemical properties of effluents

The results of physicochemical properties to tannery effluents are presented in Table 6, in which they are also been compared with the Maximum Permissible Limits in Ecuadorian Regulations [45]. Furthermore, the tannery industry provided the property values of wastewater.

The tannery effluent exceeds the maximum permissible limits, mainly in parameters such as COD and pH. In addittion, high electrical conductivity and a high total dissolved solids (TDS) value were observed, which may indicate high levels of cations representing a health problem, such as aluminum, lead, copper or arsenic [46]. Table 6 also shows the Cr(VI) result of 0.6 mg/L, which exceeds the maximum permissible limit.

3.4. Zeolite activation

The oxides were identified by XRF after activation of natural and synthetic zeolites with HCl (ZN-HCl, ZS-HCl) and NaOH (ZN-NaOH, ZS-NaOH), the results are shown in Table 7:

In ZN03, it was observed that HCl activation generated an increase in SiO_2 and a decrease in Al_2O_3; its cation exchange capacity decreased due to aluminum reduction, which reduced the sites to compensate for the excess charge, in addition to the reduction in exchangeable cations mainly due to the removal of Na^+, K^+, Mg^{2+} and Ca^{2+} cations [46]. On the other hand, activation with NaOH increased the amount of Na_2O as specific ions were eliminated and replaced with Na^+. The amount of Al increased slightly, which indicates that its cation exchange capacity would increase since it has more Na^+ and a more significant amount of exchangeable cations [23]. Based on this analysis, it can be concluded that the activation that would provide the best results for the natural zeolite is with NaOH.

The synthetic zeolite ZS01 showed that the values of P_2O_5, TiO_2, and Mn_2O_3 did not change after activation with HCl and NaOH, which indicates that these processes did not reduce the number of impurities present. The Na_2O was conserved for the activation with NaOH while it slightly decreased with HCl activation. The concentration of Al_2O_3 with HCl activation increased, while with NaOH activation, it decreased. The Si/Al ratios for synthetic zeolite, HCl-activated zeolite, and NaOH-activated zeolite were 1.60, 1.59, and 1.58, respectively. The Si/Al ratios before and after activation mostly did not change.

Table 5. Theoretical Exchange Capacity of the studied zeolites.

Zeolites	e_{Al} (eq/mol)	P_m (g/mol)	TEC (meq/100 g)	CEC (meq/100 g)
ZN03	5.7	2556.83	222.93	84.05
ZS01	4.6	950.03	484.20	188.72

e_{Al}: aluminum atoms in the zeolite formula; Pm: molecular mass of the zeolite; TEC: theoretical exchange capacity; CEC: the cation exchange capacity.

3.5. Evaluation of chromium (VI) removal with zeolite

Chromium (VI) removal tests were initially carried out with a $K_2Cr_2O_7$ solution; in all cases, the pH was regulated along with H_2SO_4 (25 % wt) to maintain the solution in a range of pH = 2 ± 0.5 [14]. The experiments were carried out with 100 ml of the chromium solution and 1 g of zeolites. The removal of Cr (VI) in the solution of 1 mg/L $K_2Cr_2O_7$

Table 6. Physicochemical properties of tannery effluents.

Parameter	Value	Maximum Permissible Limits*
pH	3.85	6.5–9
COD (mg/L)	1116	40
Electric conductivity (mS/cm)	57.9	NA
TDS (mg/L)	46320	NA
Cr (VI) (mg/L)	0.6	0.5

COD: chemical oxygen demand; TDS: total dissolved solids; * according to Ecuadorian Regulations.

Table 7. Composition of oxides (%wt) and Si/Al ratio of the natural (ZN) and synthetic (ZS) zeolites activated with HCl and NaOH.

Oxides (% wt)	ZN03	ZN03-HCl	ZN03-NaOH	ZS01	ZS01-HCl	ZN01-NaOH
SiO_2	58.08	66.21	61.56	43.44	47.84	41.63
Al_2O_3	11.04	10.93	11.15	24.04	26.59	23.25
Na_2O	0.99	<0.020	2.38	>11.00	10.47	>11.00
MgO	2.1	1.58	1.79	2.55	2.75	2.45
P_2O_5	0.19	0.11	0.17	0.06	0.06	0.06
SO_3	<0.05	<0.05	<0.05	<0.05	<0.05	<0.05
K_2O	0.7	0.53	0.51	0.65	0.71	0.55
CaO	4.84	3.19	4.66	0.44	0.52	0.46
TiO_2	0.43	0.29	0.26	0.11	0.11	0.11
Mn_2O_3	0.08	0.04	0.062	0.03	0.03	0.03
Fe_2O_3	4.25	3.99	3.95	0.73	0.8	0.71
Si/Al	**4.64**	**5.35**	**4.87**	**1.6**	**1.59**	**1.58**

Table 8. Chromium (VI) removal results from a $K_2Cr_2O_7$ solution (100 mL) using natural and activated zeolite (1 g).

Time (h)	ZN03	ZN03-NaOH	ZN03-HCl	ZS01	ZS01-NaOH
	Cr (VI) concentration (mg/L)				
0	0.7	0.7	0.7	0.9	0.9
1	0.565	0.425	0.675	0.69	0.5
2	0.51	0.265	0.635	0.50	0.415
3	0.46	0.13	0.605	0.475	0.4
Cr (VI) removal (%)	34.29	81.43	13.57	47.23	55.56

with ZN activated with NaOH was 13 %, the lowest result. The Cr(VI) concentration and the best removal results obtained with the two types of zeolites are presented in Table 8.

The removal of chromium (VI) with zeolites depends on the pH of the solution since the pH determines the selectivity of the metal ion and affects the charge of the adsorbent surface [47]. Previous work has reported that the maximum removal and adsorption capacity was at pH 1.5 [30]. Moreover, with increasing pH, the removal efficiency of Cr (VI) decreased. At acidic pH, the chromium (VI) species have a negative charge as the degree of protonation of the zeolite surface is high and the zeolite can adsorb this type of anion. If the pH is increased, the degree of protonation of the surface decreases, and the surface becomes more negative so that the adsorption decreases.

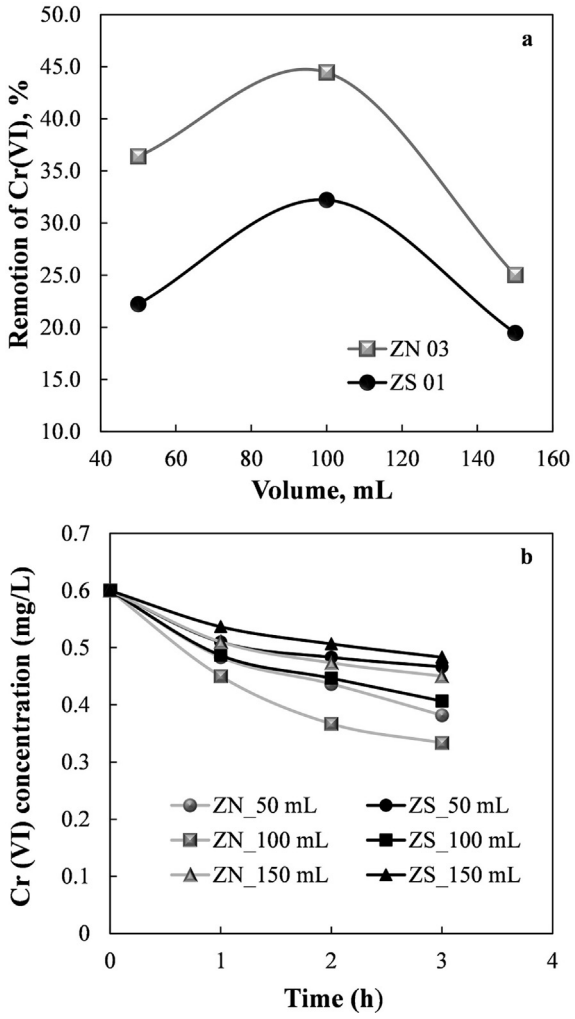

Figure 1. a) Percentage removal of Cr(VI) from tannery effluent with natural (ZN03) and synthetic (ZS01) zeolites. b) Evolution of Cr(VI) concentration as a function of removal time for the two zeolites studied. In both cases, concentrations of 0.6 mg/L and 1 g of zeolite were used.

For $K_2Cr_2O_7$ solution with a concentration of 1 mg/L of Cr (VI), removal percentages using NaOH-activated ZN were 16% compared to unactivated zeolite and HCl-activated zeolite with remotion around 10%. The NaOH-activated ZS showed an improvement in the removal of chromium (VI). Tests were not carried out with the ZS-HCl as the acid treatment increases the zeolite acidity and the effective diameter of the pores and channels. However, it produces a decrease in the ion exchange capacity, which was proven by the low percentage of removal in the natural zeolite activated with HCl [48]. From the tests performed with a $K_2Cr_2O_7$ solution, the best Cr(VI) removal percentages were obtained with natural and synthetic zeolite activated with NaOH, so these were selected for the tannery effluent tests.

The results of the percentage of Cr(VI) removal for different volumes of tannery effluent with 1g of zeolites are shown in Figure 1, in which it is evident that the two zeolites can remove Cr(VI). Figure 1a shows similar Cr(VI) removal trends between the two types of zeolite, with a maximum removal rate of 100 ml when the initial concentration of Cr(V) is 0.6 mg/L (Table 6), the agitation with 50 mL was rapid and turbulent due to its smaller volume; as a result, there was the formation of a vortex, and it is likely that there was no adequate contact between the zeolite and the effluent. This could be the reason that the adsorption did not occur successfully. Furthermore, removal decreased after 100mL as the amount of zeolite remained constant for the three volumes (1g); in addition, 100 mL greater homogenization was triggered with 250 rpm, and with 100 mL, there was a ratio of 0.01 g of zeolite/mL of effluent, which is the highest adsorbent/effluent ratio. Natural zeolite (ZN03) had a higher removal capacity than the synthetic zeolite.

Figure 1b shows the evolution of Cr(VI) concentration over time. In all experimental conditions, the Cr(VI) was removed; the removal trends were similar for both zeolites and the treated volumes of 100 and 150 mL. The most significant difference was in the volume of 150 mL, which showed a higher removal with the natural zeolite (ZN03). At the beginning, the zeolite showed the maximum adsorption as all the active sites were available, but as time passed, it decreased, and the zeolite began to saturate.

The amount of Cr(VI) retained per unit mass of adsorbent (Q_t, mg/g) as a function of process time was determined (Equation 11) [49]:

$$Q_t = (C_o - C_t) \times \left(\frac{V}{M}\right) \quad [11]$$

Co: initial metal concentration (mg/L); Ct: metal concentration at time t (mg/L); V: volume of effluent (L); M: mass of zeolite (g).

The results of quantity of chromium (Q_t) removed are presented in Table 9; the natural zeolite ZN retained the highest amount of chromium per mass of adsorbent. In addition, the amount of Cr(VI) retained increased with time.

In the previous results, the best removal option was obtained with natural zeolite activated with NaOH used for tests in fixed beds; the breakthrough curves for different quantities of zeolite beds are shown in Figure 2, which demonstrates, that the curve with the highest bed height lost adsorption capacity more slowly than the others, and the higher the bed height is related to a more significant amount of zeolite. The concentration of Cr (VI) removed increased over time, a

Table 9. Amount of Cr (VI) adsorbed of zeolite (Q_t, mg/g) for different volumen of tannery effluent.

Time (h)	V = 50 mL		V = 100 mL		V = 150 mL	
	ZN03	ZS01	ZN03	ZS01	ZN03	ZS01
1	0.0057	0.0043	0.0150	0.0113	0.0133	0.0093
2	0.0080	0.0057	0.0233	0.0153	0.0187	0.0140
3	0.0107	0.0063	0.0267	0.0193	0.0223	0.0173

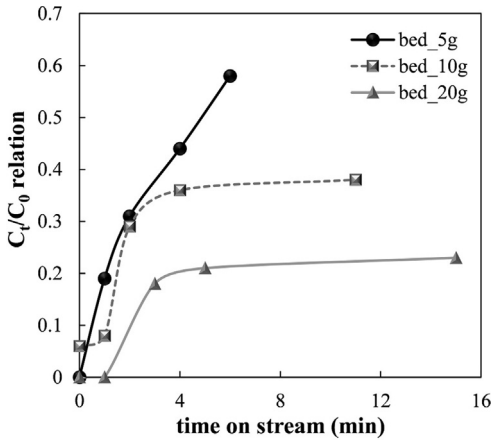

Figure 2. Cr (VI) adsorption on activated natural zeolite (ZN) for different beds.

trend that was evident in the 5 g bed. For the 10 and 20 g beds, after 6 min, the concentration reached an equilibrium point where the beds were likely saturated and no longer had the adsorbent capacity to remove Cr(VI). The curve with the highest bed height (20 g) lost adsorption capacity more slowly than the others. With a high mass of zeolite in the bed, the feed solution flowed into the column for a longer residence time which increased mass transfer [50]and caused the chromium concentration to decrease. At the initial times, all the active sites were available for chromium adsorption, which could infer that the zeolite has the maximum adsorption capacity initially, which decreases over time and when in contact with the effluent. At lower altitudes, the Cr (VI) concentration at the tower outlet increased rapidly due to the predominance of the axial dispersion effect [50, 51]; this also means that the metal ion cannot diffuse throughout the mass of the adsorbent.

4. Conclusions

On the mineralogical characterization, the natural and synthetic zeolite has a majority clinoptilolite/heulandite, and faujasite type composition, respectively, and the total exchange capacity before activation of the natural zeolite is 84.05 meq/100g and of the synthetic zeolite is 188.72 meq/100g.

In natural zeolite, activation with NaOH was better than with HCl, as NaOH promotes the removal of certain anions and their replacement with Na^+. The Si/Al ratio in the synthetic zeolite after activation with NaOH and HCl showed minimal variations, and there were no significant variations in the percentages of the constituent oxides. Preliminary tests with a synthetic Cr solution led to the conclusion that the zeolites that promote more significant removal are activated with NaOH.

The tannery effluent had a Cr (VI) concentration of 0.6 mg/L, COD 1116 mg/L and pH 3.85, values that are above the maximum permissible limit according to the Ecuadorian Environmental Regulations. Furthermore, the Cr (VI) removal tests with the effluent yielded 44.44 % removal with the ZN-NaOH and 32.22 % with the ZS-NaOH, which means that the effluent complies with the permissible Cr(VI) limit for discharge with final concentrations of 0.33 and 0.42 mg/L, respectively. For 3 h, in 100 and 150 mL of effluent, there was a removal of 0.0267 and 0.0223 mg Cr (VI)/g of ZN-NaOH respectively, and the highest adsorption was obtained in 100 mL due to the lower volume.

The amount of Cr(VI) retained per unit mass increased with time for the two zeolites, and better chromium removal results were obtained with the natural zeolite. Similar removal results were obtained when working in fixed beds, so this material could also suit this configuration. The proposed method could be scalable for tannery effluent treatment, allowing for a geological resource that has not yet been explored in Ecuador, as the zeolites.

Declarations

Author contribution statement

Ana María Álvarez: Performed the experiments. Analyzed and interpreted the data. Wrote the original draft.

Darío Bolaños Guerrón: Analyzed and interpreted the data. Wrote, edited and reviewed the paper.

Carolina Montero Calderón: Conceived the research. Analyzed and interpreted the data. Wrote, edited and reviewed the paper. Was in charge of overall direction and planning of the project. All the authors discussed and reviewed the results.

Funding statement

This research did not receive any specific grant from funding agencies in the public, commercial, or not-for-profit sectors.

Data availability statement

Data included in article/supplementary material/referenced in article.

Declaration of interests statement

The authors declare no conflict of interest.

Additional information

No additional information is available for this paper.

Acknowledgements

The authors are grateful to the Departamento de Ciencias de la Tierra y Construcción (Universidad de las Fuerzas Armadas, ESPE). A.M. Álvarez acknowledge to the closed Instituto Nacional Geológico Minero Metalúrgico del Ecuador for the lab facilities in the development to her Master's thesis. C. Montero Calderón is grateful to Facultad de Ingeniería Química (Universidad Central del Ecuador) for the research facilities. All the authors appreciate to Curtiembre La Alborada for the samples of tannery effluents.

References

[1] J. Oleas, H. Jácome, Boletín mensual de análisis sectorial de MIPYMES: Ropa de vestir de cuero para exportación, Quito, 2011.

[2] O.M. Naranjo Mantilla, L.M. Loor Mendoza, Estudio de los residuos generados en el proceso de curtido y el impacto ambiental en la Empresa Curtiduría Hidalgo, Universidad Tecnológica Indoamérica, 2017. http://repositorio.uti.edu.ec//handle/123456789/627. (Accessed 14 May 2021).

[3] A.A. Belay, Impacts of chromium from tannery effluent and evaluation of alternative treatment options, J. Environ. Prot. (Irvine,. Calif). 1 (2010) 53–58.

[4] H. Suman, V.K. Sangal, M. Vashishtha, Treatment of tannery industry effluent by electrochemical methods: a review, Mater. Today Proc. (2021).

[5] A. Fouda, S.E. Hassan, E. Saied, M.F. Hamza, Photocatalytic degradation of real textile and tannery effluent using biosynthesized magnesium oxide nanoparticles (MgO-NPs), heavy metal adsorption, phytotoxicity, and antimicrobial activity, J. Environ. Chem. Eng. 9 (2021) 105346.

[6] A.B. Mpofu, O.O. Oyekola, P.J. Welz, Anaerobic treatment of tannery wastewater in the context of a circular bioeconomy for developing countries, J. Clean. Prod. 296 (2021) 126490.

[7] S. Mustapha, M.M. Ndamitso, A.S. Abdulkareem, J.O. Tijani, A.K. Mohammed, D.T. Shuaib, Potential of using kaolin as a natural adsorbent for the removal of pollutants from tannery wastewater, Heliyon 5 (2019), e02923.

[8] J.A. Figueirôa, G.U. Menezes Novaes, H. de Souza Gomes, V.L. de Morais Silva, D. de Moraes Lucena, L.M. Lima, S.A. de Souza, L.G. Viana, L.A. Rolim, J.R. da Silva Almeida, A.P. de Oliveira, J.P. Gomes, Opuntia ficus-indica is an excellent eco-friendly biosorbent for the removal of chromium in leather industry effluents, Heliyon 7 (2021), e07292.

[9] Y.A. Neolaka, E.B. Kalla, G. Supriyanto, N. Nyoman Tri Puspaningsih, Adsorption of hexavalent chromium from aqueous solutions using acid activated of natural zeolite collected from Ende-Flores, Indonesia, RASAYAN J. Chem. 10 (2017) 606–612.

[10] H. Nigam, M. Das, S. Chauhan, P. Pandey, P. Swati, M. Yadav, A. Tiwari, Effect of chromium generated by solid waste of tannery and microbial degradation of chromium to reduce its toxicity: a review, Adv. Appl. Sci. Res. 6 (2015) 129–136. www.pelagiaresearchlibrary.com. (Accessed 14 May 2021).

[11] L. Sivarama Krishna, K. Soontarapa, A. Yuzir, V.A. Kumar, W.Y. Zuhairi, Kaolin-nano scale zero-valent iron composite(K-nzvi): synthesis, characterization and application for heavy metal removal, Desalin. Water Treat. 100 (2017) 168–177.

[12] L. Sivarama Krishna, K. Soontarapa, N.K. Asmel, M.A. Kabir, A. Yuzir, W.Y. Wan Zuhairi, Y. Sarala, Adsorption of acid blue 25 from aqueous solution using zeolite and surfactant modified zeolite, Desalin. Water Treat. 150 (2019) 348–360.

[13] J.S. Marciano, R.R. Ferreira, A.G. de Souza, R.F.S. Barbosa, A.J. de Moura Junior, D.S. Rosa, Biodegradable gelatin composite hydrogels filled with cellulose for chromium (VI) adsorption from contaminated water, Int. J. Biol. Macromol. 181 (2021) 112–124.

[14] M. Forghani, A. Azizi, M.J. Livani, L.A. Kafshgari, Adsorption of lead(II) and chromium(VI) from aqueous environment onto metal-organic framework MIL-100(Fe): synthesis, kinetics, equilibrium and thermodynamics, J. Solid State Chem. 291 (2020) 121636.

[15] Y. Cao, S. Dong, Z. Dai, L. Zhu, T. Xiao, X. Zhang, S. Yin, M.R. Soltanian, Adsorption model identification for chromium (VI) transport in unconsolidated sediments, J. Hydrol. 598 (2021) 126228.

[16] S.K. Lakkaboyana, K. Soontarapa, Vinaykumar, R.K. Marella, K. Kannan, Preparation of novel chitosan polymeric nanocomposite as an efficient material for the removal of Acid Blue 25 from aqueous environment, Int. J. Biol. Macromol. 168 (2021) 760–768.

[17] S.K. Lakkaboyana, S. Khantong, N.K. Asmel, A. Yuzir, W.Z. Wan Yaacob, Synthesis of copper oxide nanowires-activated carbon (AC@CuO-NWs) and applied for removal methylene blue from aqueous solution: kinetics, isotherms, and thermodynamics, J. Inorg. Organomet. Polym. Mater. 29 (2019) 1658–1668.

[18] L. Sivarama Krishna, K. Soontarapa, N.K. Asmel, A. Yuzir, W.Y. Wan Zuhairi, Effect of cetyltrimethylammonium bromide on the biosorption of acid blue 25 onto bengal gram fruit shell, Desalin. Water Treat. 150 (2019) 386–395.

[19] S.K. Lakkaboyana, K. Soontarapa, N.K. Asmel, V. Kumar, R.K. Marella, A. Yuzir, W.Y. Zuhairi, Synthesis and characterization of Cu(OH)2-NWs-PVA-AC Nano-composite and its use as an efficient adsorbent for removal of methylene blue, Sci. Rep. 11 (2021) 1–17.

[20] N.K. Asmel, A.R.M. Yusoff, L. Sivarama Krishna, Z.A. Majid, S. Salmiati, High concentration arsenic removal from aqueous solution using nano-iron ion enrich material (NIIEM) super adsorbent, Chem. Eng. J. 317 (2017) 343–355.

[21] L. Machiels, D. Garcés, R. Snellings, W. Vilema, F. Morante, C. Paredes, J. Elsen, Zeolite occurrence and genesis in the Late-Cretaceous Cayo arc of Coastal Ecuador: evidence for zeolite formation in cooling marine pyroclastic flow deposits, Appl. Clay Sci. 87 (2014) 108–119.

[22] P.K. Huanca, B. Paredes, M. Rodríguez, D.P. Gonzales, T.R. Tejada, J.E. Chávez, Caracterización y aplicación de una zeolita natural de ocuviri (Perú) para la remoción de Pb (ii) en solución a nivel laboratorio, Av. En Ciencias e Ing 9 (3) (2018) 1–12. ISSN-e 0718-8706, https://dialnet.unirioja.es/servlet/articulo?codigo=6597220&info=resumen&idioma=ENG. (Accessed 14 May 2021).

[23] F.E. Morante Carballo, Las zeolitas de la costa de Ecuador (Guayaquil) : geología, caracterización y aplicaciones, E.T.S.I. Minas (UPM), 2017.

[24] M. Medina González, Y. Redondo Naranjo, Validación de la determinación de la capacidad de intercambio catiónico total, método del cloruro de amonio, IV Congr. Cuba, Min. IV Simp. Minería y Metal (2011).

[25] G. Fipps, Irrigation Water Quality Standards and Salinity Management Strategies, 2003.

[26] W. and A. American Water Works Association (AWWA), Standard Methods for the Examination of Water and Wasterwater, 23rd ed., American Public Health Association (APHA), 2017. https://www.wef.org/resources/publications/books/StandardMethods/. (Accessed 19 May 2021).

[27] J.C. Gil Solano, Tratamiento electroquímico para la remoción de metales pesados en residuos líquidos peligrosos generados en los laboratorios de docencia de la Universidad del Cauca, Universidad del Valle, 2014. https://bibliotecadigital.univalle.edu.co/handle/10893/7642. (Accessed 25 July 2021).

[28] Y. Yulianis, S. Muhammad, K. Pontas, M. Mariana, M. Mahidin, Characterization and activation of Indonesian natural zeolite from southwest aceh district-aceh province, in: IOP Conf. Ser. Mater. Sci. Eng., Institute of Physics Publishing, 2018, 012052.

[29] M. Djaeni, L. Kurniasari, A. Purbasari, S.B. Sasongko, Activation of natural zeolite as water adsorbent for mixed-adsorption drying, in: Proceeding 1st Int. Conf. Mater. Eng. 3rd AUN/SEED-Net Reg. Conf. Mater., 2010. http://www.foxitsoftware.com. (Accessed 14 May 2021).

[30] J.Y. Hamdo Hommaid, Adsorption of chromium(VI) from an Aqueous Solution on a Syrian Surfactant-Modified Zeolite, 2014.

[31] M. Panayotova, Possible Use of Metal -modified Clinoptilolite for Chromium Removal from Wastewater, 2020. https://obuch.info/possible-use-of-metal.html. (Accessed 14 May 2021).

[32] L. Manrique Losada, N.C. Bonilla, R. Chica Buitrago, J.H. Otálora Bonilla, M. Salamanca, Estudio preliminar de la Capacidad de Remoción de Iones inorgánicos de Una zeolita sintética tipo faujasita, Rev. Fac. Ciencias Básicas. 11 (2016) 114.

[33] G. Du, Z. Li, L. Liao, R. Hanson, S. Leick, N. Hoeppner, W.T. Jiang, Cr(VI) retention and transport through Fe(III)-coated natural zeolite, J. Hazard Mater. 221–222 (2012) 118–123.

[34] J. Lemus, J. Soler, M.P. Pina, Influencia del cation de intercambio y de relación Si/Al en zeolitas como conductores protónicos para su uso en pilas PEMFC de alta temperatura, 2007.

[35] P. Sáez González, Eliminación de metales estratégicos en aguas residuales mediante adsorción con zeolitas naturales, Universidad Complutense de Madrid, 2021.

[36] J. Alvarado Ibarra, Caracterización de una chabasita natural sonorense y evaluación de su potential para utilizarse en la remoción de metales en agua, Universidad de Sonora, 2014. http://repositorioinstitucional.uson.mx/handle/unison/522. (Accessed 25 July 2021).

[37] International Zeolite Association, Database of Zeolite Structures, 2021. https://america.iza-structure.org/IZA-SC/ftc_table.php. (Accessed 14 May 2021).

[38] S. V Boycheva, D.M. Zgureva, Surface Studies of Fly Ash Zeolites via Adsorption/desorption Isotherms, 2016.

[39] M. Jiménez, Caracterización de minerales zeolíticos mexicanos, Universidad Autónoma del Estado de México, 2004.

[40] M.A. Hernández, F. Rojas, V.H. Lara, R. Portillo, G. Pérez, R. Salas, Estructura porosa y propiedades estructurales de mordenita y clinoptilolita, Superf. y Vacío. 23 (2010) 51–56. https://www.redalyc.org/articulo.oa?id=94248264011. (Accessed 18 May 2021).

[41] D.B. Mosqueda Jiménez, Estudios de zeolitas naturales y modificadas para su utilización como catalizadores de control ambiental, Tecnológico de Monterrey, 1997. https://repositorio.tec.mx/handle/11285/569915. (Accessed 18 May 2021).

[42] M. Rodríguez, Valdivia, Evaluacion de la capacidad de adsorción de NH^{4+} y metales pesados Pb^{2+}, Cd^{2+}, Cu^{2+}, Zn^{2+} y Mn^{2+} empleando zeolitas naturales y sinteticas, Universidad Nacional de San Agustín de Arequipa, 2017. http://repositorio.unsa.edu.pe/handle/UNSA/4515. (Accessed 18 May 2021).

[43] B.I. El-Eswed, Aluminosilicate inorganic polymers (geopolymers): emerging ion exchangers for removal of metal ions, in: Appl. Ion Exch. Mater. Environ., Springer International Publishing, 2019, pp. 65–93.

[44] M. Jeeva, S.K. Lakkaboya, W.Y. Wan Zuhairi, The adsorption of direct brown 1 dye using kaolinite and surfactant modified kaolinite, Bull. Geol. Soc. Malays. (2019) (2019) 47–57.

[45] Ministerio Del Ambiente, Ecuador, Norma de Calidad Ambiental y de Descarga de Efluentes, Recurso Agua, Ecuador, 2015.

[46] R. Vela Vázquez, Mejora de propiedades adsortivas de la zeolita tipo chabasita para la captura de CO_2 de post combustión, Benemérita Universidad Autónoma de Puebla, 2019. https://repositorioinstitucional.buap.mx/handle/20.500.12371/4725. (Accessed 18 May 2021).

[47] P.K. Pandey, S.K. Sharma, S.S. Sambi, Kinetics and equilibrium study of chromium adsorption on zeolitenax, Int. J. Environ. Sci. Technol. 7 (2010) 395–404.

[48] M.A. Jurado Eraso, Estudio de la desaluminización post síntesis de una zeolita tipo A, Universidad Nacional de Colombia, 2004. https://repositorio.unal.edu.co/handle/unal/2692. (Accessed 18 May 2021).

[49] F. Granados-Correa, J. Serrano-Gómez, Removal of chromium hexavalent ions from aqueous solution by retention onto iron phosphate, J. Chil. Chem. Soc. 55 (2010) 312–316.

[50] C.R. Girish, V.R. Murty, Adsorption of phenol from aqueous solution using lantana camara, forest waste: packed bed studies and prediction of breakthrough curves, Environ. Process. 2 (2015) 773–796.

[51] R.E. Treybal, Operaciones De Transferencia De Masa, second ed., McGraw-Hill, 1988.